

## **Sensitivity analysis of a stress strain model for steel fiber reinforced concrete plates**

Fernando LOPEZ-GAYARRE\*, Alberto DOMINGO<sup>a</sup>, Carlos LÁZARO<sup>a</sup>, Miguel A. SERRANO<sup>b</sup>, María PELUFO<sup>a</sup>

\*Dep. Construction. University of Oviedo  
Campus de Viesques, 33203. Gijón, Spain  
gayarre@uniovi.es

<sup>a</sup> ETSICCP. Polytechnic University of Valencia.

<sup>b</sup> Dep. Construction. University of Oviedo

### **Abstract**

This article deals with the sensitivity study of a given model for the behavior of thin laminar elements of SFRC (steel fiber reinforced concrete). In order to carry out this analysis, a brief description of the model used for the behavior of the SFRC in laminar elements is presented. The analysis was made by means of ABAQUS finite element software with a particular model for the behavior of SFRC. The limit of the fragile-plastic behavior of SFRC plates has been established as an outcome of the analysis. The results of test performed on plates were compared with the numerical simulation. Good correlation between experimental results and those obtained in the numerical simulation was observed as an adequate support for the model.

**Keywords:** SFRC, finite elements analysis, stress-strain model, toughness indexes.

### **1. Introduction**

A sensitivity analysis of the model given by Domingo [1] is proposed for the behavior of the concrete reinforced with steel fibers in thin laminar elements. This model considers three stages in the tensile behavior of the SFRC. The first stage corresponds to an elastic and linear behavior of the SFRC before cracking and is defined by the elastic moduli and the tensile strength of the concrete matrix  $\sigma_t$ . The second branch corresponds to a linear decrease caused by the occurrence of the first crack reaching up to 0.02 mm ( $\epsilon_{w0}$ ), as in Hillerborg [2], but it stops due to the presence of fibers and the mobilization of the residual stress  $\sigma_r$  generating the beginning of the third branch from which the SFRC develops its corresponding ductile behavior, expressed by means of a nearly horizontal straight line with a 0.1% slope. **Figure 1** shows the corresponding model.

**Figure 1** also shows the main parameters of the model. These parameters are: the maximum tensile strength before cracking ( $\sigma_t$ ), the elastic moduli of the SFRC ( $E$ ), the residual stress ( $\sigma_f$ ) and the strain ( $\epsilon_{w0}$ ).

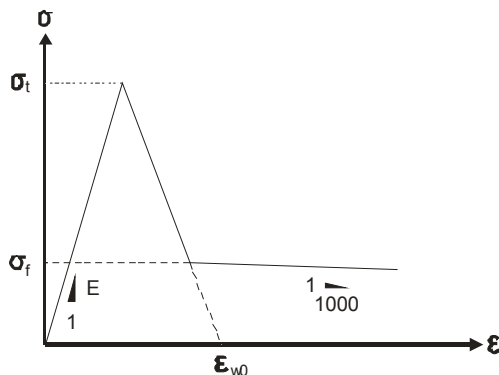


Figure 1: Proposed model for tensile behavior of the SFRC.

The sensitivity analysis will be focused on the maximum tensile strength and the residual stress. Similarly, analysis of several toughness indexes and toughness will be made, assuming toughness as the area under the load versus relative displacement curve measured up to a value of the relative displacement equal to 1/150 of the distance between the plate supports, as in JSCE [3], [4].

Within this article the results of the experimental analysis of SFRC plates will be presented. They are relevant for the discussion of the model's sensitivity.

The sensitivity analysis was made through the implementation of the model in the ABAQUS/Standard software.

This study confirms and verifies the applicability of the proposed model for the behavior of thin plates of SFRC and offers a greater support for this model. In addition, it explains the behavior of the load–displacement curve in a deeper way so as to understand the influence of each one of this curve parameters in the behavior of the concrete reinforced with steel fibers in laminar structures and, thus, to determine if it is possible to consider this concrete as a fragile or ductile material in its structural application.

## 2. Experimental program.

As part of the experimental program made by A. Domingo [1], [5] for obtaining the model's main parameters and its validation, it was proposed to make tests in thin plates (1.20×1.20×0.06 m) with different fiber contents. Within these plate tests three different load systems were included: (a) a load system that generates a state of uniaxial bending forces, (b) a load system that generates a state of biaxial bending forces that is equal in two

perpendicular directions and (c) a state of biaxial bending forces that is unequal in two perpendicular directions.

**Figures 2, 3 and 4** show the load systems proposed for the tests. The position of the seven vertical displacement sensors remains unchanged in the three load systems. **Figure 5** shows the position of these sensors corresponding to the points at which the load is applied. The load is applied using a hydraulic jack. During the tests the applied load and the measurement of the displacement sensors are registered continuously.

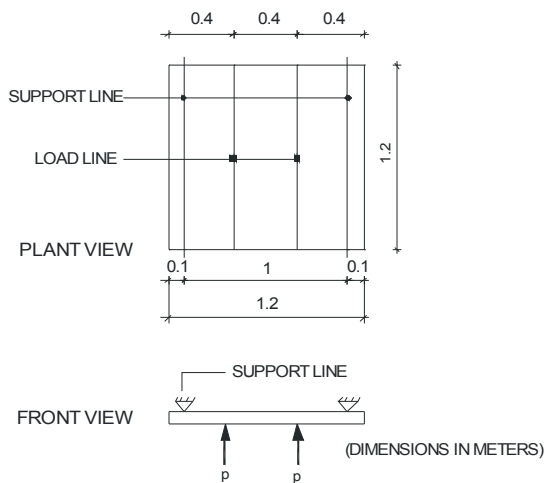


Figure 2: First load system

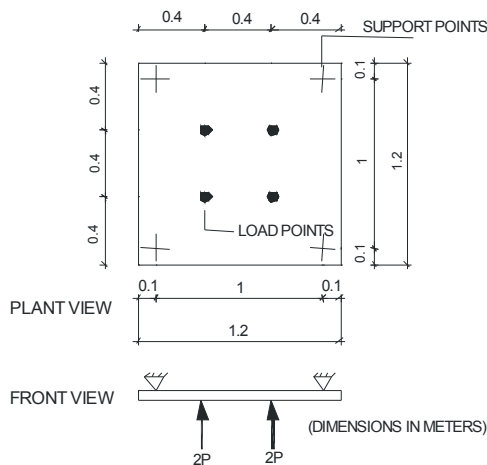


Figure 3: Second load system

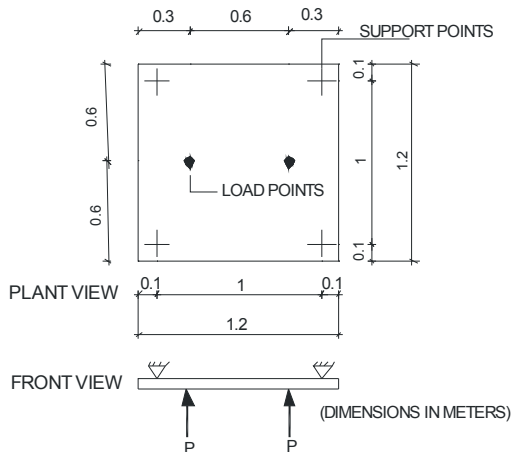


Figure 4: Third load system

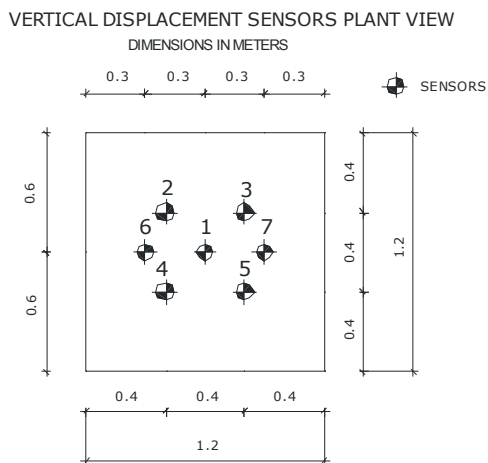


Figure 5: Position of the vertical displacement sensors

For these tests, toughness and different toughness indexes were also measured. Furthermore, after implementing the model's behavior in a finite elements software, the theoretical results for the toughness value and the different toughness indexes were checked against the experimental data.

**Figures 6, 7 and 8** show the results obtained experimentally for the toughness and toughness indexes for the three load systems, and **figures 9, 10 and 11** show these values obtained through the ABAQUS software. It was observed a good agreement between the model and the experimental results regarding the toughness and its associated indexes.

Fibers kg/m <sup>3</sup>	Displ. 1° fracture mm	I <sub>5</sub>	I <sub>10</sub>	I <sub>20</sub>	I <sub>30</sub>	Toughness up to 2.6 mm N·m	Average of toughness N·m
50	0.2856	5.141	10.119	20.294	—	44.872	41.276
	0.4393	4.822	9.396	—	—	37.681	
	0.4860	4.253	—	—	—	*	
70	0.0839	3.374	6.835	15.379	21.019	49.868	58.488
	0.2045	7.935	18.973	49.063	69.562	63.285	
	0.4314	4.428	8.395	15.441	21.865	53.691	
90	0.3717	5.874	12.811	27.297	35.116	60.564	60.564
	0.1375	5.043	10.294	21.171	—	*	
*plates that did not reach 2.6 mm.							

Figure 6: Toughness indexes and toughness up to a displacement of 2.6 mm - Plates tested with the first load system.

Fibers kg/m <sup>3</sup>	Displ. 1° fracture	I <sub>5</sub>	I <sub>10</sub>	I <sub>20</sub>	I <sub>30</sub>	Toughness up to 2.6 mm N·m	Average of toughness N·m
50	0.2878	5.067	10.007	—	—	*	36.264
	0.1679	—	—	—	—	*	
	0.1517	4.466	10.101	19.755	28.888	36.264	
70	0.2778	3.783	7.395	15.005	21.936	52.917	52.609
	0.2436	5.701	11.533	—	—	*	
	0.2158	4.506	7.969	14.844	21.406	52.300	
90	0.2064	5.011	10.199	21.070	25.513	54.159	54.159
	0.0839	5.702	12.123	—	—	*	
*plates that did not reach 2.6 mm.							

Figure 7: Toughness indexes and toughness up to a displacement of 2.6 mm - Plates tested with the second load system.

Fibers kg/m <sup>3</sup>	Displ. 1° fracture mm	I <sub>5</sub>	I <sub>10</sub>	I <sub>20</sub>	I <sub>30</sub>	Toughness up to 2.6 mm N·m	Average of toughness N·m
50	0.1232	3.433	7.252	15.318	22.391	34.414	30.939
	0.0952	5.358	10.544	20.838	30.973	27.464	
70	0.0326	4.961	9.989	20.014	29.176	34.044	35.587
	0.1498	5.039	10.552	22.343	34.117	43.129	
90	0.2141	4.668	9.583	19.157	28.884	39.748	42.214
	0.1373	5.733	12.005	25.491	39.032	44.679	

Figure 8: Toughness indexes and toughness up to a displacement of 2.6 mm - Plates tested with the third load system

Fibers kg/m <sup>3</sup>	Displ. 1° fracture: mm	I <sub>5</sub>	I <sub>10</sub>	I <sub>20</sub>	I <sub>30</sub>	Toughness up to 2.6 mm N·m
50	0.1888	3.342	6.241	12.007	17.818	37.773
70	0.1282	3.930	7.667	15.156	22.930	58.008
90	0.1127	4.351	8.622	17.335	26.922	70.009

Figure 9: Toughness indexes and toughness up to a displacement of 2.6 mm with the model proposed for the first load system

Fibers kg/m <sup>3</sup>	Displ. 1° fracture: mm	I <sub>5</sub>	I <sub>10</sub>	I <sub>20</sub>	I <sub>30</sub>	Toughness up to 2.6 mm N·m
50	0.1880	3.560	6.594	12.634	18.745	36.732
70	0.2239	3.918	7.627	15.171	22.886	49.569
90	0.2604	3.847	7.530	15.168	—	52.89

Figure 10: Toughness indexes and toughness up to a displacement of 2.6 mm with the model proposed for the second load system

Fibers kg/m <sup>3</sup>	Displ. 1° fracture: mm	I <sub>5</sub>	I <sub>10</sub>	I <sub>20</sub>	I <sub>30</sub>	Toughness up to 2.6 mm N·m
50	0.1163	3.571	6.753	13.364	20.234	28.799
70	0.2069	4.380	8.686	17.849	27.386	38.606
90	0.2001	4.631	9.333	19.352	29.825	41.604

Figure 11– Toughness indexes and toughness up to a displacement of 2.6 mm with the model proposed for the third load system.

### 3. Sensitivity study of model.

The analysis of the model's sensitivity was focused solely in parameters  $\sigma_t$  and  $\sigma_f$ , in order to evaluate its possible influence in the final results of the model. The variation of the elastic moduli has not been considered, since this parameter has little variation for concrete coming from the same mix; on the other hand, its determination can be carried out in a very precise way by means of standardized laboratory tests.

In this study it was decided in addition to consider the toughness indexes listed below, where each index depends on the magnitude of the relative displacement corresponding to the first fracture, which must be obtained from tests load-displacement curves.

I<sub>5</sub>: Relation between the area under the load versus relative displacement curve up to 3 times the relative displacement in the first fracture, and the area up to this relative displacement where the first fracture appears.

I<sub>10</sub>: Relation between the area under the load versus relative displacement curve up to 5.5 times the relative displacement in the first fracture, and the area until this relative displacement where the first fracture appears.

I<sub>20</sub>: Relation between the area under the load versus relative displacement curve up to 10.5 times the relative displacement in the first fracture, and the area until this relative displacement where the first fracture appears.

I<sub>30</sub>: Relation between the area under the load versus relative displacement curve up to 15.5 times the relative displacement in the first fracture, and the area until this relative displacement where the first fracture appears.

The sensitivity study was carried out on the base of the second load system, verifying that in the other two load systems their behavior was analogous. The following ranges of variation for the parameters<sup>1,2</sup> were considered (in MPa):

$$2.25 \leq \sigma_t \leq 3.50$$

$$1.20 \leq \sigma_f \leq 2.00$$

With these data, a very wide range of values for the tensile strength of the concrete are covered. The values of the residual stress correspond to concrete with enough fiber content

for the considered plates. In **figure 12** each one of the twenty five analyzed possibilities are identified. Their behavior, in each case, was analyzed by means of ABAQUS/Standard.

TEST	$\sigma_t$ MPa	$\sigma_f$ MPa	TEST	$\sigma_t$ MPa	$\sigma_f$ MPa	TEST	$\sigma_t$ MPa	$\sigma_f$ MPa
1	2.25	1.2	10	2.5	2	19	3	1.8
2	2.25	1.4	11	2.71	1.2	20	3	2
3	2.25	1.65	12	2.71	1.4	21	3.5	1.2
4	2.25	1.8	13	2.71	1.65	22	3.5	1.4
5	2.25	2	14	2.71	1.8	23	3.5	1.65
6	2.5	1.2	15	2.71	2	24	3.5	1.8
7	2.5	1.4	16	3	1.2	25	3.5	2
8	2.5	1.65	17	3	1.4			
9	2.5	1.8	18	3	1.65			

Figure 12: Tests for the sensitivity study

## 4. Analysis and results.

### 4.1 Influence of the residual stress.

Initially the influence analysis of the residual stress was made in the load–displacement curve. **Figures 13 to 17** show the load versus relative displacement curves, arranged so that all the curves in each graph correspond to behaviors with the same first crack strength, but with different residual stress.

These graphs show a rigid initial behavior up to the first crack load. The curves corresponding to lower residual stress show a sudden fall of the load after fracture, and a later stabilization with an almost horizontal and slightly increasing trend with load levels below the peak load. On the contrary, for higher levels of residual stress, after the first fracture occurrence the capacity to support increasing loads continues, although with less rigidity and it was observed that the bigger strength to first fracture is the greater the demand of residual stress is to obtain an elasto-plastic behavior.



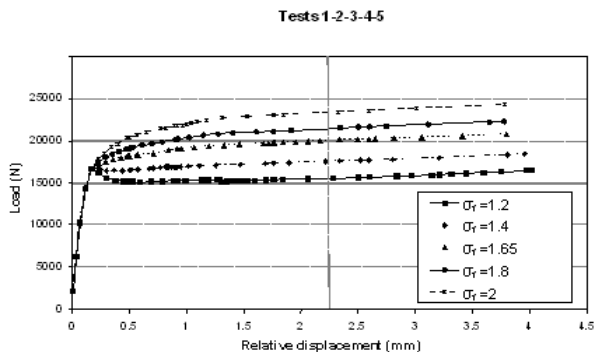


Figure 13: Load versus relative displacement,  $\sigma_t = 2.25$  MPa.

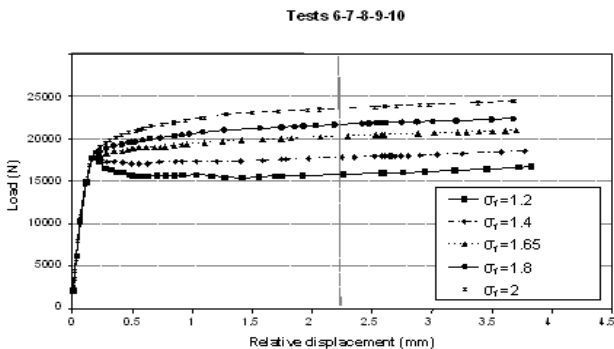


Figure 14: Load versus relative displacement,  $\sigma_t = 2.50$  MPa.

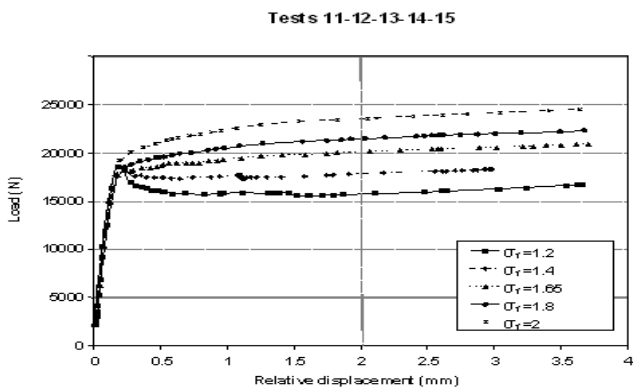


Figure 15: Load versus relative displacement,  $\sigma_t = 2.71$  MPa.

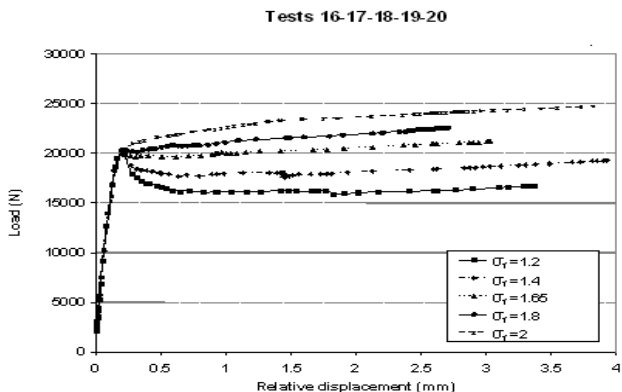


Figure 16: Load versus relative displacement,  $\sigma_t = 3.00$  MPa.

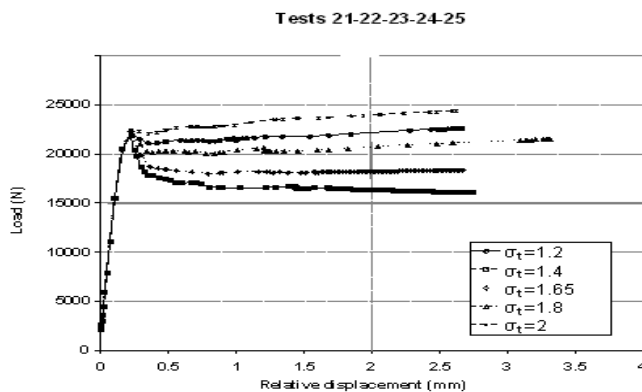


Figure 17: Load versus relative displacement,  $\sigma_t = 3.50$  MPa.

#### 4.2 Influence of stress at first fracture.

Figures 18 to 22 show the load versus relative displacement curves, displayed in a way that all the curves in each graph correspond to behaviors with the same residual stress, but with different strengths to first fracture.

From these figures it can be concluded that the stress variations to first fracture have influence on the branch next to the peak. The post-cracking behavior, with a practically constant load level, is similar for all the concretes with the same residual stress, thus, all curves tend to reach similar load levels.

The concretes of lower residual stress show a peak, which will be more significant for better matrix quality. Therefore, the fragile behavior will be more sensitive to variations of the matrix strength.

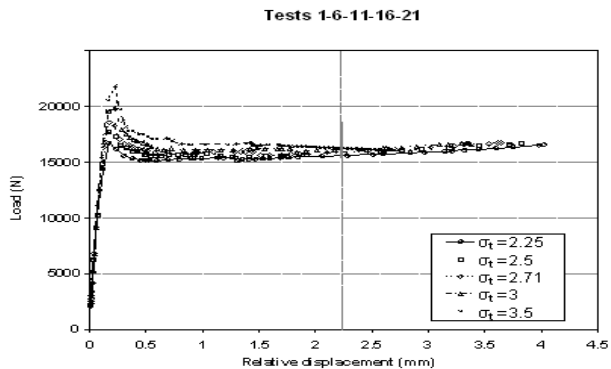


Figure 18: Load versus relative displacement,  $\sigma_f = 1.20$  MPa.

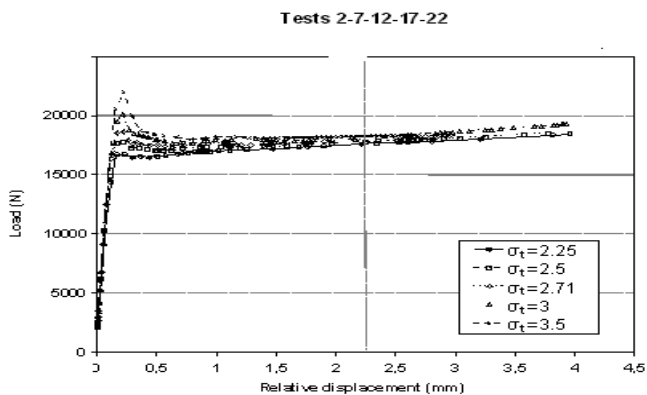


Figure 19: Load versus relative displacement,  $\sigma_f = 1.40$  MPa.

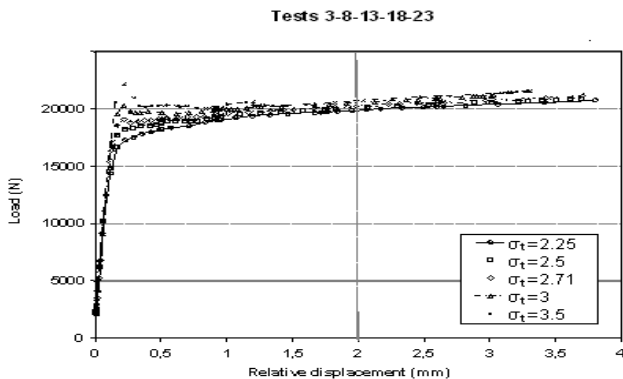


Figure 20: Load versus relative displacement,  $\sigma_f = 1.65$  MPa.

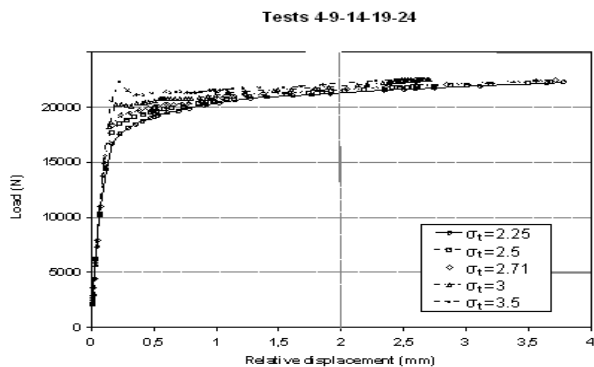


Figure 21: Load versus relative displacement,  $\sigma_f = 1.80$  MPa.

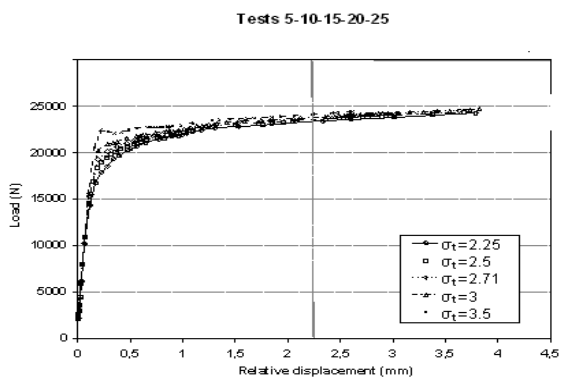


Figure 22: Load versus relative displacement,  $\sigma_f = 2.00$  MPa.

### 4.3 Evolution of toughness and toughness indexes.

Figure 23 shows the toughness variation based on the residual stress for different values of the tensile strength, measured in energy units (Area under the load versus relative displacement curve up to a displacement equal to 1/150 of the distance between plate supports). This graph shows a general increase of the toughness versus to the residual stress; an important increase of the residual stress (69%) produces a low increase of the toughness (37%). Regarding to the toughness indexes, analyses of the variations based on the parameters used were made and the obtained results showed very small variations for the different cases analyzed.

The effect of the first fracture is less important, since a great increase of the tensile strength (55%) produces a very small variation of toughness (6%).

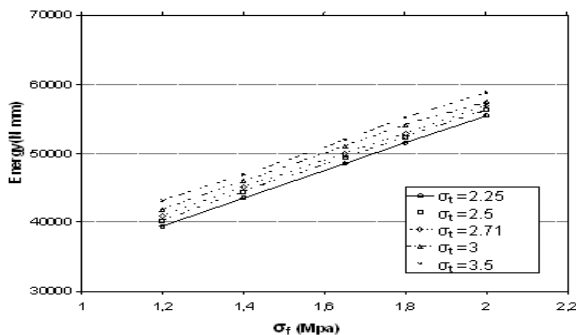


Figure 23: Toughness trend curves versus to  $\sigma_f$

## 5. Conclusions.

It is possible to manufacture a ductile SFRC for plates concrete modifying the relation  $\sigma_t/\sigma_f$ . In this way, it seems that there is a limit in the relation between tensile strength  $\sigma_t$  and residual stress  $\sigma_f$ , that marks off the fragile-plastic behavior from the elastic-plastic behavior.

The toughness and the toughness indexes increase when the residual stress grows up.

Furthermore it was also observed that  $\sigma_t$  does not influence significantly in the toughness value nor in the load value necessary to reach a certain displacement.

In addition, the variation of the tensile strength does not influence over the ultimate load, i.e., the increase of the maximum tensile strength does not involve higher ultimate loads.

On the other hand, if for each value of the tensile strength is plotted the range of variation of the residual stress in which the change of the fragile behavior to the elastic-plastic behavior takes place, the limit of the shell's ductile behavior is obtained. **Figure 24** shows the result of this analysis, displaying the range of residual stress in which the change of the shell behavior takes place. Within this range the limit was determined as:

$$\sigma_f = 0.5 \sigma_t + 0.3 \text{ (MPa)}$$

For  $\sigma_f$  values lower to the ones provided in the previous relation, the shell behavior curves display a prominent cracking peak with a fragile fall and a later plastic behavior. For the opposite case, they show a development of the cracking in a distributed and progressive way.

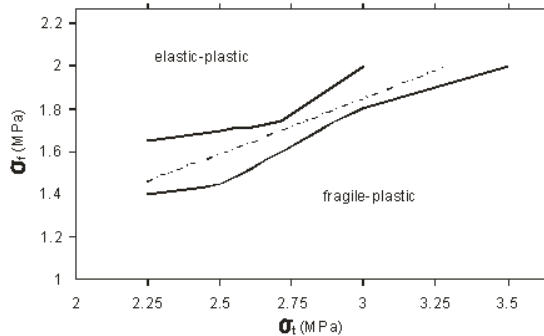


Figure 24: Limit of the plate ductile behavior.

## 6. References

- [1] Domingo, A.; Lázaro, C.; Serna, P.; "Use of steel fiber reinforced concrete in thin shell structures: evaluation of fiber performance through testing of shell specimens"; *Computational Methods*; Athens, Greece; 2000.
- [2] Hillerborg, A.; Modéer, M.; Peterson, P. E.; "Analysis of crack formation and crack growth by means of fracture mechanics and finite element"; *Cement and Concrete Research*, Vol. 6, No.6, pp. 773-781; Nov. 1976.
- [3] JSCE; "Method of Test for Steel Fiber Reinforced Concrete"; Standard JSCE-SF4 for Flexural and Flexural Toughness of SFRC and Standard JSCE-SF5 for Compressive Strength and Compressive Toughness of SFRC, *Concrete Library of JSCE, Japan Society Civil Engineers*, N. 3, pp. 58: 66; June 1984.
- [4] JSCE-SF4; "JSCE-SF4: method of tests for flexural strength and flexural toughness of steel fiber-reinforced concrete"; *Concrete library of JSCE, Vol. 3, Japan Society of Civil Engineers (JSCE)*, pp. 63-66; Tokyo; 1984.
- [5] Domingo, A.; Lázaro, C.; Serna, P.; "Using a postfailure stress-displacement material model for SFRC plates. Evaluation through testing of shell specimens"; *International symposium on Theory, Design and Realization of Shell and Spatial Structures, IASS*, H. Kinieda; Nagoya, Japan; 2001.